Two-dimensional quantum antiferromagnet with a fourfold degenerate dimer ground state

Alain Gellé,[1] Andreas M. Läuchli,[2] Brijesh Kumar,[3] and Frédéric Mila[1]
[1]*Institute of Theoretical Physics, École Polytechnique Fédérale de Lausanne, CH 1015 Lausanne, Switzerland*
[2]*Institut Romand de Recherche Numérique en Physique des Matériaux (IRRMA), CH-1015 Lausanne, Switzerland*
[3]*School of Physical Sciences, Jawaharlal Nehru University, New Delhi 110067, India*
(Received 24 April 2007; revised manuscript received 22 October 2007; published 15 January 2008)

We study the competition between antiferromagnetic order and valence-bond-crystal formation in a two-dimensional frustrated spin-1/2 model. The J_1-J_2 model on the square lattice is further frustrated by introducing products of three-spin projectors which stabilize four dimer-product states as degenerate ground state. These four states are reminiscent of the dimerized singlet ground state of the Shastry-Sutherland model. Using exact diagonalization, we study the evolution of the ground state by varying the ratio of interactions. For a large range of parameters ($J_2 \gtrsim 0.25 J_1$), our model shows a direct transition between the valence-bond-crystal phase and the collinear antiferromagnetic phase. For small values of J_2, several intermediate phases appear which are also analyzed.

DOI: 10.1103/PhysRevB.77.014419 PACS number(s): 75.10.Jm, 75.30.Kz, 75.50.Ee, 75.40.Mg

I. INTRODUCTION

In the last several years, a large amount of work has been devoted to the study of quantum systems with frustrated magnetic interactions due to their propensity to present spin liquid states. These phases indeed present interesting low energy properties, starting with the absence of magnetic order even at zero temperature. Recently, a lot of attention has been focused particularly on the valence bond crystal (VBC) states, and more precisely on the transition between these states and a magnetically ordered phase. In this context, it has been suggested[1,2] that this could be a second order transition which does not belong to the Landau-Ginsburg paradigm.[3]

In a VBC state, spins are coupled in pairs forming singlet states, evocating valence bonds. These pairwise singlets are themselves arranged in a periodic pattern. Such states break the translation symmetry, and it is possible to define an order parameter quantifying the singlet long range order. The question on the nature of quantum phase transition that separates this state from a long-range ordered magnetic phase is very interesting as well as current. Supposing a second order transition within the Landau-Ginsburg paradigm,[3] the order parameters of both phases should vanish precisely at the transition. Intuitively, it seems more probable that the two order parameters will not vanish exactly at the same point, leading either to a first order transition, or to two second order transitions separated by an intermediate phase. For a spin-1/2 system on square lattice, Senthil and co-workers have recently suggested an alternative scenario of second order phase transitions that are not described by Landau-Ginsburg theory.[1,2] The transition could instead be described by means of fractional degrees of freedom, namely spinons. These spinons become deconfined at the transition point, called the deconfined quantum critical point.

A priori, the spin-1/2 J_1-J_2 antiferromagnet on square lattice seems to be the simplest choice to investigate the relevance of this new scenario. Here, J_1 and J_2 denote the strengths of first and second neighbor spin interactions. In the two limiting cases where either J_1 or J_2 is very large compared to the other, the system presents antiferromagnetic order. In the former case it corresponds to the usual Néel order, and in the latter case the ground state has a collinear antiferromagnetic order, corresponding to the Néel order on two sublattices (that are obtained by connecting second neighbor sites). It is generally accepted that this model presents an intermediate spin disordered phase in the range $0.4 \lesssim J_2/J_1 \lesssim 0.6$, which might break the translational symmetry.[4–10] It is still unclear if the transition between the Néel state and the spin disordered phase is a deconfined quantum critical point or a simple first order transition, although recent works are in favor of a weak first order transition.[11–13]

The difficulty in understanding the J_1-J_2 model comes from the intermediate phase whose nature is subject to discussions.[14] Some studies show a four-spin plaquette order,[9,10] while others are in favor of a columnar dimer order.[6–8] In the latter case, not only the translational symmetry, but also the fourfold lattice rotational symmetry is broken. However, if this phase develops dimer-dimer correlations, it is far away from being the simple direct product of dimer singlet wave functions. Indeed, if that was the case, the ground state would present a strong signal of long-range dimer order which is not observed for the intermediate phase of the J_1-J_2 model. Exact diagonalization studies show that the dimer-dimer correlation is rapidly decreasing with distance[6,15] and that, if the dimer order exists, it should be rather small.[15] The analysis of the properties of the phase transition is therefore not so easy in the J_1-J_2 model. Recently, a new model including ring-exchange has been proposed[16] to explore the possibility of non Landau-Ginsburg phase transitions. It has however been shown that this model presents a first order transition.[16] On the other hand, Sandvik explored an SU(2) symmetric ring-exchange-like model on square lattice, and found strong numerical evidence in favor of a true deconfined quantum critical point.[17]

In the present paper, we propose a quantum spin-1/2 model on square lattice with frustrated antiferromagnetic interactions. Interestingly, for a simple choice of the interaction parameters, this model has an exactly solvable singlet ground

 ©2008 The American Physical Society

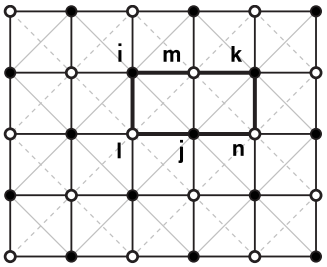

FIG. 1. Representation of a 3 by 2 horizontal rectangular plaquette. A vertical 2 by 3 plaquette can be obtained by a 90° rotation of the plaquette. Solid and dashed gray lines represent A and B sublattices. Spins are represented by black and white dots for sublattices A and B, respectively.

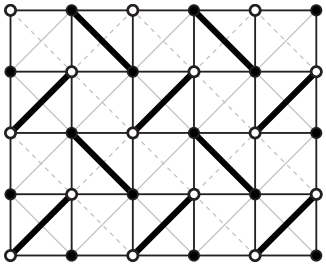

FIG. 2. One of the four VBC configurations in the ground state of H_0. Thick black lines indicate the pairs of spins that form singlet states. The three other ground states can be obtained by translation of the dimer pattern by lattice vectors.

state. The exact ground state is a pure direct product of dimers, arranged in the same pattern as in the ground state of the Shastry-Sutherland model.[18] However, unlike in the Shastry-Sutherland model, the VBC ground state of our model presents a case of spontaneous symmetry breaking, and is fourfold degenerate, in agreement with field-theory arguments.[19,20] Using exact diagonalization, we investigate the evolution of the ground state as the interaction parameters are varied away from the exactly solvable VBC case. In the following section, we describe the model and discuss its main properties and its relation to the J_1-J_2 model. In Sec. III A, we study the competition between the VBC phase and the collinear ordered antiferromagnetic phase. In Sec. III B, we analyze the competition with the usual Néel antiferromagnetic phase. Finally, the last section is devoted to conclusions and perspectives.

II. MODEL

Consider a system of spin-1/2 on the square lattice. The model we consider contains only two and four spins interactions which can be conveniently described using a six-site rectangular plaquette (see Fig. 1). It is also convenient to distinguish between the two sublattices A and B of the square lattice. The six sites of a plaquette thus contain three sites belonging to A sublattice, and the other 3 sites belonging to B sublattice. For each set of three spins, we consider the spin projector on the quartet $(S=3/2)$ state

$$P^A_{i,j,k} = \frac{1}{3}\left[(\vec{S}_i + \vec{S}_j + \vec{S}_k)^2 - \frac{3}{4}\right], \tag{1}$$

$$P^B_{l,m,n} = \frac{1}{3}\left[(\vec{S}_l + \vec{S}_m + \vec{S}_n)^2 - \frac{3}{4}\right], \tag{2}$$

where A and B refer to the two sublattices, and i,j,k,l,m,n are the sites of the plaquettes as depicted in Fig. 1. The interaction we consider is obtained by taking the product of two projectors of a plaquette

$$H_0 = \sum_{[i,j,k,l,m,n]} \frac{9}{4} P^A_{i,j,k} P^B_{l,m,n}, \tag{3}$$

where the sum runs over all horizontal and vertical plaquettes and $[i,j,k,l,m,n]$ are the sites of one plaquette.

One should notice that the value of a projector is always positive except when the three spins are in a doublet state [i.e., when $(\vec{S}_i+\vec{S}_j+\vec{S}_k)^2=3/4$], in this case it becomes zero. The latter condition is fulfilled, in particular, if any two of the three spins form a singlet. These two spins could either be two first neighbor or two second neighbor spins of a sublattice, and correspond, respectively, to two second or two third neighbor spins of the original square lattice. Since the interaction in the model is the product of two projectors, it is only necessary to cancel one of these projectors to minimize the corresponding term. For this purpose, it is thus sufficient to have one dimer on the plaquette, either between second or third neighbor spins. Therefore, it is obvious that if a valence bond configuration has one such dimer on every plaquette, it will form a zero energy ground state of H_0.

Historically, the original case of stabilizing valence bond states by spin projectors was presented in the Majumdar-Ghosh model on a spin-1/2 chain.[21] Motivated by this work, Klein proposed a general scheme of constructing quantum spin models with exact dimer ground states, going beyond one dimension (1D).[22] Though Klein's method uses the theory of symmetric group for constructing models with dimerized ground states, these constructions can be conveniently described in terms of the spin projection operators introduced by Löwdin.[23] Encouraged by Klein's approach, several model Hamiltonians have been derived on different types of 2D lattices.[24] Some of these investigations were done in order to find spin models that could be accurately described by the quantum dimer model of Rokhsar and Kivelson.[25] There have been several other studies, inspired by Majumdar-Ghosh model, in which various exactly solvable spin models with dimer ground states were constructed in different spatial dimensions (some of which have extensive entropy in the exact dimer ground state).[26] Recently, Batista and Trugman studied a model with such projectors on four-site square plaquettes[16] but their Hamiltonian has a highly degenerate ground state since a great number of dimer patterns minimize all projectors.

In the present model, the ground state is obtained when dimers are arranged in the pattern given in Fig. 2 and is much less degenerate (see also the discussion in the Appendix). This arrangement evokes the Shastry-Sutherland (SS) model (and we will further refer to this phase as the SS-VBC phase), but contrary to the SS model, our Hamiltonian does

not break the translational symmetry of the square lattice. The ground state presents a spontaneous symmetry breaking, and is fourfold degenerate. The other three of SS-VBC states can be obtained from this dimer pattern by simple lattice-translations. Interestingly, the four SS-VBC states are also the exact zero energy eigenstates (although not the ground state) of the nearest-neighbor Heisenberg model on square lattice, which motivated us to seek for a model on the square lattice with four SS-VBC states as the exact ground state.[27]

The spin projectors are two-spin operators which can be rewritten in terms of the exchange couplings between the first and second neighbor spins of a sublattice

$$P^A_{i,j,k} = \frac{2}{3}(\vec{S}_i \cdot \vec{S}_j + \vec{S}_i \cdot \vec{S}_k + \vec{S}_j \cdot \vec{S}_k) + \frac{1}{2}. \tag{4}$$

Therefore, the product of two projectors generates two- and four-spin interactions in H_0. Since the projector is invariant under spin-rotation and involves spins on a given sublattice, it will commute with the total spin of this sublattice, and obviously, with the total spin of the other sublattice. H_0 will thus conserve the total spin on each sublattice. This extra symmetry can introduce a further factor two in the degeneracy of excited states.

It is interesting to notice that this Hamiltonian is somehow related to the J_1-J_2 model. Let us assume that a state can be expressed as a direct product of the wavefunction of spins on A sublattice $|\Psi_A\rangle$ and of spins on B sublattice $|\Psi_B\rangle$:

$$|\Psi\rangle = |\Psi_A\rangle \otimes |\Psi_B\rangle. \tag{5}$$

In that case, it is possible to define a Hamiltonian for one sublattice. Let us, for instance, choose the A sublattice

$$H_A = \sum_{[i,j,k,l,m,n]} \frac{9}{4} P^A_{i,j,k} \langle \Psi_B | P^B_{l,m,n} | \Psi_B \rangle. \tag{6}$$

This Hamiltonian corresponds, for the A sublattice, to a model with first and second neighbor interactions whose amplitudes are modulated by the local spin state of the B sublattice. It is easy to show that, in the case where the mean value of the projector on B sublattice is homogeneous, the Hamiltonian can be expressed as

$$H_A = 3\langle P^B \rangle \sum_{\langle i,j \rangle_A} \vec{S}_i \cdot \vec{S}_j + \frac{3}{2}\langle P^B \rangle \sum_{\langle\langle i,j \rangle\rangle_A} \vec{S}_i \cdot \vec{S}_j, \tag{7}$$

where $\langle i,j \rangle_A$ are the first neighbor couples of spins of A sublattice, and $\langle\langle i,j \rangle\rangle_A$ the second neighbor ones, $\langle P^B \rangle$ is the uniform value of $\langle \Psi_B | P^B_{l,m,n} | \Psi_B \rangle$. This Hamiltonian is precisely the J_1-J_2 model on the A sublattice at the $J_2/J_1 = 0.5$ point, which is located in the intermediate spin liquid phase of the model. Clearly, if we consider the ground state of our model, we do not expect the mean value of the P^B projector to be homogeneous. Nevertheless, this comparison introduces a simple picture of the model, in which the local spin correlations self-consistently modulate the J_1-J_2 model on each sublattice. This process allows the system to stabilize a pure direct product of dimers as ground state. This valence bond ground state is different in nature from the one expected in the intermediate phase of J_1-J_2 model, since the dimer order on each sublattice is not columnar but staggered[28] (see Fig. 2).

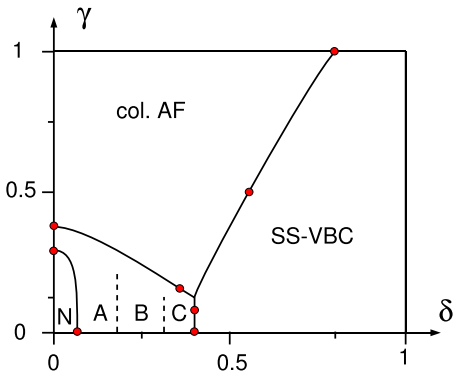

FIG. 3. (Color online) Tentative phase diagram of the model (8). Phase transitions obtained by exact diagonalizations of the present work are indicated by full dots. These points have been obtained from finite size scaling analysis of the order parameters, except for those at the transition between *SS-VBC* and *C* phases. The latter transition correspond to a level crossing. The points correspond to the position of the crossing obtained for the largest cluster size. Phase transitions in dashed line are estimations based on the crossing of preponderant Q dependent magnetic structure factors (see Fig. 10). The nature of the different phases is described in the following sections. The points on the $\delta=0$ line are taken from Ref. 4.

The existence of this exact ground state makes this model an interesting candidate to explore the transition between the VBC phase and the antiferromagnetically ordered state. In order to drive the system into such phases, we consider the following Hamiltonian:

$$H = J(1-\gamma)(1-\delta)\sum_{\langle i,j \rangle} \vec{S}_i \cdot \vec{S}_j + J\gamma(1-\delta)\sum_{\langle\langle i,j \rangle\rangle} \vec{S}_i \cdot \vec{S}_j + J\delta H_0, \tag{8}$$

where $\langle i,j \rangle$ and $\langle\langle i,j \rangle\rangle$ are, respectively, first and second neighbor spins of the original (square) lattice, γ and δ are dimensionless parameters, and J is the energy scale (assumed to be positive). When δ is equal to 1, one just retrieves the H_0 model, while when $\delta=0$, the Hamiltonian is simply the J_1-J_2 model, with γ being equal to $J_2/(J_1+J_2)$. A sketch of the phase diagram of the Hamiltonian (8) is shown in Fig. 3. It contains three unambiguously identified phases denoted by "N" [antiferromagnetic (π,π) Néel order], "col. AF" [collinear $(\pi,0)/(0,\pi)$ order with Néel order each sublattice], and "SS-VBC" (valence-bond order with Shastry-Sutherland arrangement). Between these phases, there is a region where correlations change very significantly, defining possible phase transitions between three phases denoted by A, B, and C. These phases are discussed in the last part of the next section.

III. NUMERICAL RESULTS

We study the evolution of the eigenstates of this model by an exact diagonalization technique based on the Lanczos algorithm. Finite clusters of $N=16$, 20 and 32 sites were used.

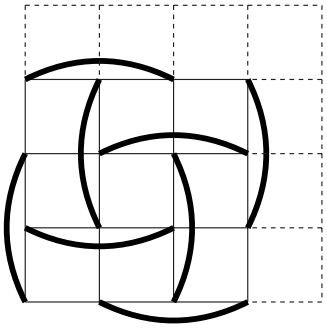

FIG. 4. Representation of one of the two additional ground states for the 16 site cluster. Full lines connect the 16 sites of the cluster, dashed lines symbolize the boundary conditions. The other additional ground state can be obtained by translation of the dimer pattern by lattice vectors.

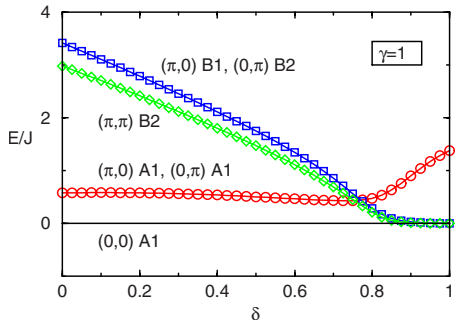

FIG. 5. (Color online) Energy differences between the ground state and some of the lower states of the 32 site cluster. The symmetry of different states is indicated in the figure. Values in parenthesis correspond to momentum, while $A1$, $B1$, $A2$, and $B2$ refer to the irreducible representations of the point group symmetry. For $(0,0)$ and (π,π) momentum the point group is C_{4v}, and for $(\pi,0)$ momenta it is C_{2v}. A (respectively, B) notation indicates that the state is symmetric (respectively, antisymmetric) under $\pi/2$ rotation for C_{4v} or π rotation for C_{2v}. The last number corresponds to the reflection symmetries. $A1$ (respectively $A2$) states are symmetric (respectively antisymmetric) under reflections, while for $B1$ and $B2$ it depends on the axis. States with $(\pi,0)$-A_1 and $(0,\pi)$-A_1 symmetry are triplet states, others are singlet states.

Larger clusters were not accessible because of the complexity of the interaction.

The first noticeable result concerns $\delta=1$ case, when $H=JH_0$. We checked numerically that the four SS-VBC ground states presented in previous section are the only ground states of the model. This is always true except for the 16 site cluster, for which two more ground states are also present, as shown in Fig. 4. These two states are ground states only for the 16 site cluster, due to the very short loops which wrap around the boundaries of the cluster (also see the Appendix). Indeed, in this case a third neighbor dimer between the sites (x,y) and $(x,y+2)$ also represents a dimer between the sites $(x,y+2)$ and $(x,y+4)$ because of the periodic boundary conditions. This is no longer true for larger clusters and by extension in the thermodynamic limit.

In the following two subsections, we map out the phase diagram of the model, with an emphasis on two lines: first the case of $\gamma=1$, studied in Sec. III A and, secondly, $\gamma=0$, presented in Sec. III B. The former line connects the case of $J_1=0$, $J_2=J$ and $\delta=0$ to the fourfold degenerate SS-VBC ground state, and the latter connects the unfrustrated square lattice Heisenberg antiferromagnet to the same dimerized ground state.

A. SS-VBC versus collinear order ($\gamma=1$)

In the present section, we consider the case where $\gamma=1$. According to the previous discussion on the relation between our model and the J_1-J_2 model, J_2 corresponds to a first neighbor interaction on each sublattice which, for large enough values, will lead to a Néel state on each sublattice.

For $\delta=1$, the SS-VBC states are exact ground states even for finite clusters. Note that these four states are nonorthogonal on a finite cluster: they have a finite overlap that decreases exponentially with the cluster size.[29] However, since they are linearly independent, the ground state is indeed fourfold degenerate on a finite cluster for $\delta=1$. This degeneracy is lifted by the J_2 interaction that appear for $\delta<1$. Figure 5 presents the energy differences between the ground state and the lowest state of some symmetry sectors, obtained for the 32 site cluster. The energy differences between the four lowest singlet states stay relatively small in the range $0.8<\delta\leq 1$, while the spin gap progressively decreases. Below 0.8 the energy difference between singlet states rapidly increases, while the spin gap remains approximately constant. The fact that the spin gap is close to its $\delta=0$ value (i.e., the value of the J_1 model) suggests that the system is in the corresponding antiferromagnetic phase, and hence that it will have a zero spin gap in the thermodynamic limit.

In order to further investigate the transition, we calculate the $\vec{Q}$ dependent magnetic susceptibility for each cluster[32]

$$M_N^2(\vec{Q}) = \frac{1}{N(N+2)} \sum_{i,j} \langle \vec{S}_i \cdot \vec{S}_j \rangle e^{i\vec{Q}(\vec{r}_j - \vec{r}_i)}, \tag{9}$$

where $\vec{r}_i$ denotes the position of ith spin, $\langle \cdots \rangle$ the expectation value in the ground state, and N the number of sites in the cluster. The evolution of the $\vec{Q}_1=(\pi,0)$ magnetic susceptibility relevant for antiferromagnetic collinear order is presented in Fig. 6. The extrapolation to the thermodynamic limit of the corresponding sublattice magnetization[4] has been performed using the finite size scaling predicted by nonlinear sigma model studies[30,31]

$$M_N^2(\vec{Q}_1) = \frac{1}{8} m_0^2(\vec{Q}_1) + \frac{\text{const}}{\sqrt{N}}. \tag{10}$$

The fitted value of $m_0(\vec{Q}_1)$ is also shown in Fig. 6. The extrapolated magnetization stays large up to $\delta \simeq 0.7$, which confirms that the collinear phase is stable in this range of parameter. It then rapidly drops, and vanishes around $\delta \approx 0.75$.

The VBC phase, which is expected for larger values of δ, is characterized by long range dimer-dimer correlation. This long range correlation can be considered as the order param-

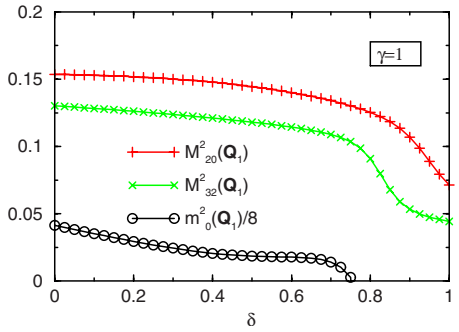

FIG. 6. (Color online) $M_N(\vec{Q}_1)^2$ square magnetic susceptibility for 20 and 32 site clusters $[\vec{Q}_1=(\pi,0)]$ and its extrapolation to the thermodynamic limit $M_\infty(\vec{Q}_1)^2=m_0^2(\vec{Q}_1)/8$.

eter of this symmetry-breaking phase. In order to determine the stability of the phase, we compute the following dimer-dimer correlations in the ground state:

$$D_N(\vec{r}) = \langle(\vec{S}_{\vec{0}}\cdot\vec{S}_{\vec{r}_1})(\vec{S}_{\vec{r}}\cdot\vec{S}_{\vec{r}+\vec{r}_2})\rangle - \langle\vec{S}_{\vec{0}}\cdot\vec{S}_{\vec{r}_1}\rangle\langle\vec{S}_{\vec{0}}\cdot\vec{S}_{\vec{r}_2}\rangle, \quad (11)$$

where $\vec{0}$ stands for the origin, and $\vec{r}_1$ and $\vec{r}_2$ can be either equal to $(1,1)$, $(1,-1)$, $(-1,1)$, or to $(-1,-1)$. As expected, for $\delta\sim 1$, the values of $D(\vec{r})$ that correspond to the dimers of the Shastry-Sutherland pattern are quite large. For a given cluster, and close to $\delta=1$, the fluctuations of these values are very small, of the order of a few percent of the average value of these correlations. Since we are interested in the value of $D(\vec{r})$ for r going to infinity, we only considered among these correlations the one obtained for the largest r value $[D_N(\vec{r}_m)]$. These correlations, shown in Fig. 7, are quite small in the antiferromagnetic phase, and rapidly increase at around $\delta\sim 0.8$. Interestingly enough, the curves cross at $\delta=0.76$, very close to the point where the antiferromagnetic order vanishes. This behavior is consistent with a first order transition, with an order parameter scaling down to zero with the cluster size below a critical value, and scaling up to a finite value above. However, with only two sizes available (the 16 site cluster turns out to be rather pathological with essentially δ

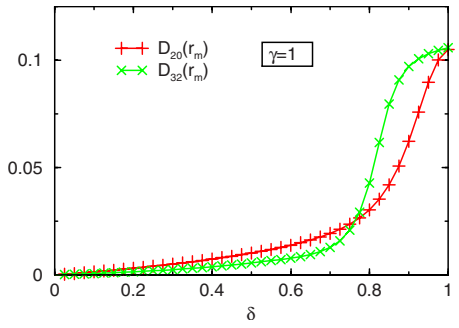

FIG. 7. (Color online) Dimer-dimer correlation D_m/D_0 obtained for the 20 and 32 site cluster. This value corresponds for one cluster to the correlation between the two dimers of the Shastry-Sutherland pattern separated by the largest distance. $D_0=3^3/4^4$ is the maximal correlation obtained for a pure fourfold degenerate dimer state.

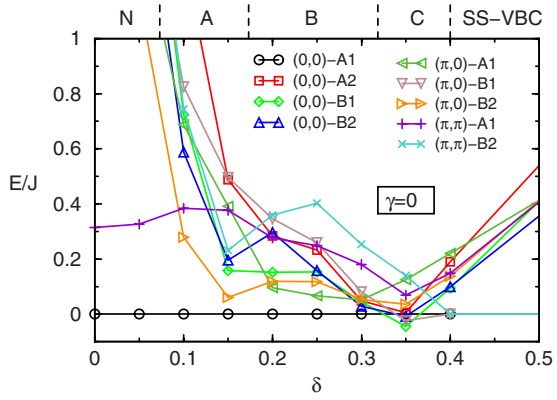

FIG. 8. (Color online) Energy differences between the lowest fully symmetric state with $\vec{k}=(0,0)$ momenta and some of the lowest states of the 32 site cluster. The labeling of the symmetry sectors follows the caption of Fig. 5.

independent correlations), this information should be taken with care, and a definitive identification of the nature of the phase transition requires further investigation.

B. Competition with (π,π) Néel order ($\gamma=0$)

We now consider the case of $\gamma=0$, which corresponds to the competition between the first neighbor coupling and the six site plaquette interaction. The interest in the model obtained for $\gamma=0$ comes from the fact that the SS-VBC states remain eigenstates for all values of δ with an energy equal to zero. It follows that the transition at which the valence-bond-crystal vanishes has to be a level crossing and is therefore first order.

In the case discussed in the previous section, we argued that the transition between the collinear $(\pi,0)$ Néel phase and the SS-VBC could in principle be a continuous transition. A very simple observation in this direction is the fact that both phases rely on strong antiferromagnetic spin correlations between second neighbor spins. This is no longer the case for (π,π) Néel order which is stabilized by the nearest-neighbor coupling J_1 $(\gamma=0,\delta=0)$, and therefore presents strong antiferromagnetic correlations between nearest neighbor spins and ferromagnetic correlations between second neighbor spins, hinting at a severe reorganization of the wavefunction between the Shastry-Sutherland VBC and the (π,π) Néel phase. According to this simple consideration, a direct transition between the SS-VBC phase and the (π,π) Néel phase seems unlikely. In the following, we will see that these observations are indeed corroborated by the results of the numerical simulations.

We start the discussion by presenting in Fig. 8 the evolution of the energies of some of the lowest eigenstates obtained for the 32-site cluster, taking the lowest fully symmetric $\vec{k}=(0,0)$ level as the energy reference. To identify intermediate phases present in the range $0.1\lesssim\delta\lesssim 0.4$, we searched for predominant signals in either the real space dimer-dimer correlations or the momentum dependent magnetic structure factor (see Fig. 10). Due to the difficulty in performing a finite-size scaling of the order parameters, this

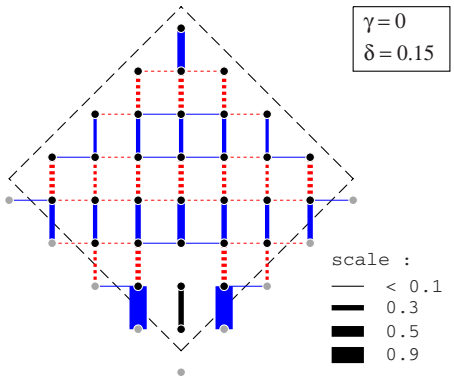

FIG. 9. (Color online) Correlations between first neighbor spin dimers [see Eq. (12)] on the 32 site cluster for $\gamma=0$ and $\delta=0.15$ (phase A). Positive values are represented by (blue) plain lines, and negative values by (red) dashed lines. The thickness is proportional to the relative amplitude D_m/D_0 of the correlation as depicted on the figure ($D_0=3^3/4^4$ is the maximum of correlation obtained for a pure fourfold degenerate dimer state). The (black) dimer in the lowest corner of the cluster is the reference dimer.

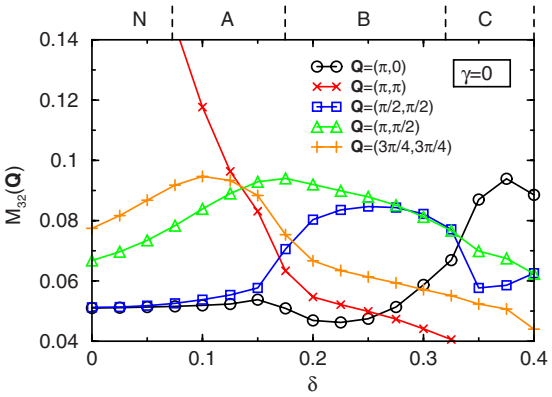

FIG. 10. (Color online) Q-dependent magnetic structure factor obtained for the 32 site cluster.

identification of the phases as well as the transition points has a preliminary character at this stage, and is mainly based on the qualitative differences of structure factors and energy level orderings as one tunes δ from 0 to 0.4. Based on this analysis, we are led to propose three different phases, tentatively labeled as "A," "B," and "C" in addition to the well characterized (π,π) Néel phase at $\delta=0$ and the fourfold degenerate Shastry-Sutherland states for $\delta\gtrsim 0.4$. We discuss each of these three additional phases in the following, starting with the phase "A" adjacent to the (π,π) Néel order at small δ, continuing with the phase "C" adjacent to the exact Shastry-Sutherland eigenstates at $\delta\lesssim 0.4$, and concluding with the elusive region "B" in between.

Phase "*A*". Starting at small values of δ, we note that the plaquette interactions favor antiferromagnetic correlations between second neighbor spins, similar to a frustrating AF J_2 coupling. Therefore one could expect the evolution of the system to be similar to the J_1-J_2 model for intermediate values of J_2. The symmetry of the four lowest states near $\delta=0.15$ with momenta $(0,0)$ (two states), $(\pi,0)$, and $(0,\pi)$, are indeed compatible with the hypothesis of a fourfold degenerate ground state with a translational symmetry breaking of the columnar dimer type, although the energetic separation of these four states with respect to the higher levels has not been achieved yet. Figure 9 shows for $\delta=0.15$ the following nearest neighbor dimer-dimer correlations:

$$D_N(\vec{r}) = \langle (\vec{S}_0 \cdot \vec{S}_{\vec{r}_3})(\vec{S}_{\vec{r}} \cdot \vec{S}_{\vec{r}+\vec{r}_4}) \rangle - \langle \vec{S}_0 \cdot \vec{S}_{\vec{r}_3} \rangle \langle \vec{S}_0 \cdot \vec{S}_{\vec{r}_4} \rangle, \quad (12)$$

where this time $\vec{r}_3$ and $\vec{r}_4$ can be either equal to $(0,1)$, $(0,-1)$, $(1,0)$, or $(-1,0)$. These correlations are relatively large and long ranged through the sample, and provide support for valence bond ordering of the nearest neighbor dimers. However, one should note that, as for the J_1-J_2 model, it is difficult to determine whether this phase presents columnar dimer order or plaquette order in the thermodynamic limit.[14] So based on the properties of the spectrum and the presence of sizable dimer correlations we suggest the presence of a phase "*A*" which forms some sort of valence bond crystal based on dimers on nearest-neighbor bonds. The transition point between this phase and the Néel phase *N* has been evaluated by computing the finite size scaling of the staggered magnetic structure factor (not shown). This structure factor, which corresponds to the order parameter squared of the Néel phase, vanishes at about $\delta=0.06$.

Phase "*C*". At the other end of the δ axis, starting from large values of δ, the ground state stays exactly fourfold degenerate down to $\delta\simeq 0.4$, below which a level crossing occurs. Note that in Fig. 8 at $\delta=0.4$ the levels $(0,0)$-$A1$ (one dimensional), $(\pi,0)$-$B1$ (two dimensional), and (π,π)-$B2$ (one dimensional) are exactly degenerate. Near $\delta=0.35$ many levels are very close in energy. Some of these states are even found to be lower in energy than the fully symmetric $\vec{k}=(0,0)$ state, which is again the ground state for $\delta\leq 0.3$, but this may well be a finite size effect on this particular sample.

For $\gamma=1$ studied in Sec. III A, we encountered a direct transition between a collinear $(\pi,0)$ Néel ordered phase and the Shastry-Sutherland–type VBC state. In order to rule out this scenario here, we determined the static spin structure factors for different momenta in Fig. 10. At a first glance the $(\pi,0)$ components seem strongest around $\delta\sim 0.35$. In order to shed further light on the absence of magnetic long range order we study the evolution of the collinear magnetic order as a function of γ for a fixed value of $\delta=0.35$. Using samples of 20 and 32 sites we obtain in Fig. 11 a finite size scaling which shows convincingly that the magnetic order is lost at a finite value of $\gamma\sim 0.1$, i.e., the point $\delta=0.35$, $\gamma=0$ indeed does not sustain magnetic long-range order.

Looking at real-space spin correlations, the second neighbor correlation is much larger than all other spin correlations, so that the possibility of a dimer VBC state needs to be considered. We therefore computed the real-space dimer-dimer correlations which are presented in Fig. 12(a). They present a pattern reminiscent of the SS-VBC phase, although the values of the correlations are considerably smaller than in the pure phase. For the purpose of comparison, the same correlations in the pure SS-VBC phase are displayed in Fig. 12(b). We recall at this stage that in this range of parameters

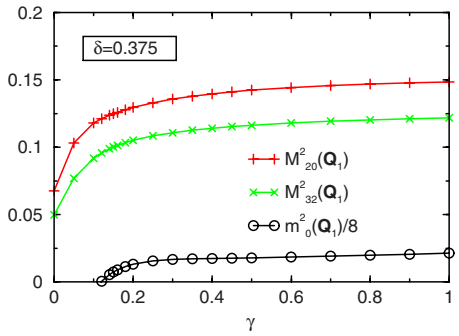

FIG. 11. (Color online) $M_N^2(\vec{Q}_1)$ square magnetic susceptibility for 20 and 32 site clusters and its extrapolation to thermodynamic limit $M_\infty(\vec{Q}_1)^2=m_0^2(\vec{Q}_1)/8$, calculated for the lowest state with momenta $\vec{k}=(0,0)$ and highest symmetry.

several states are very close in energy (see Fig. 8), all of them singlets. We also observed that they present similar dimer-dimer correlations. From our results it is however difficult to determine if these dimer-dimer correlations are short or long ranged. It seems presently as though this phase should be best visualized by a condensation of singlet excitations above the SS ground states, and not by a simple level crossing into a new ground state of completely different character, as it happens, for example, in the original Shastry-Sutherland model (Ref. 33). The nature of this phase formed by the condensing singlet levels is currently not understood.

Phase "*B*". Upon close inspection of Fig. 10 it is reasonable to suppose that there exists a third phase in the approximate region $0.2 \lesssim \delta \lesssim 0.3$—sandwiched between the phases "*A*" and "*C*"—which displays somewhat enhanced magnetic correlations for $Q=(\pi,\pi/2)$ and $Q=(\pi/2,\pi/2)$. Unfortunately the presence of correlations at these wavevectors renders the study of this parameter range more difficult, since these momenta are not present on the 20 site cluster. It is therefore not possible to perform a finite size scaling of the $\vec{Q}$-dependent magnetic structure factor. Nevertheless, one should note that there is also an enhancement of these components on the 16 site cluster. While the structure factors seem to be somewhat small for a true long-ranged spin order, these correlations still signal the presence of rather different magnetic correlations compared to the adjacent phases. Perhaps a detailed study of a classical version of the present Hamiltonian might shed some light on the possible magnetic structure which could be hidden in this region of parameter space. At this stage, it is difficult to characterize this phase "*B*" and to know if these large components correspond to a long-range spin order, or to some more exotic (e.g., nematic) phase.

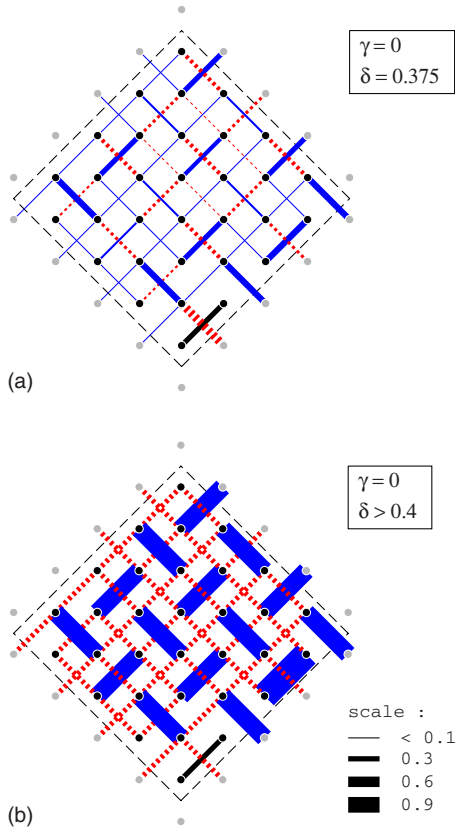

FIG. 12. (Color online) Representation of correlations between second neighbor spin dimers [see Eq. (11)] on the 32 site cluster calculated for the lowest state with momenta $\vec{k}=(0,0)$ and highest symmetry, (a) for $\gamma=0$ and $\delta=0.375$, (b) for $\gamma=0$ and $\delta>0.4$. The conventions are the same as in Fig. 9

IV. CONCLUSION

We introduced a model with frustrated interactions which provides an interesting case of competition between antiferromagnetic orders and a valence-bond-crystal order. We have shown that, for some values of the interaction parameters, the fourfold degenerate VBC ground state is an exact direct product of the dimer singlet wave functions. This model is thus an interesting candidate for investigating the possibility of a newly proposed scenario of quantum phase transition. It indeed presents, for a large range of parameters (namely, $\gamma > 0.2$), a direct transition between the SS-VBC phase and a collinear antiferromagnetic phase. Further investigations are needed to determine if the transition is first order, or if it could correspond to the non-Landau-Ginsburg transition proposed by Senthil and co-workers.[1,2]

For smaller values of the second neighbor interaction (i.e., small values of γ), the Néel and SS-VBC phases are separated by an intermediate region where different types of correlations dominate depending on the value of δ. It is likely that these correlations are the traces of intermediate phases, but further work is clearly needed to fully characterize these phases and the nature of the transitions between them.

ACKNOWLEDGMENTS

We acknowledge the support of the Swiss National Fund and of MaNEP. B.K. would like to acknowledge the DST (India) for financial assistance under the Project No. SR/FTP/PS-06/2006. The exact diagonalization computations have been enabled by allocation of resources on the IBM Regatta machines of CSCS Manno (Switzerland).

APPENDIX

The Hamiltonian H_0 [Eq. (3) of Sec. II] has four zero energy SS-VBC singlet configurations forming an exact ground state. Proving (in a mathematically rigorous way) that these four SS-VBC states are the only states in the ground state and there exists no fifth state, is a nontrivial and hard task. We are not going to attempt it here. Historically, for the Majumdar-Ghosh model, which is considerably simpler as compared to H_0, it was already very hard to prove the exact twofold degeneracy of the ground state [which was eventually shown by AKLT (Ref. 34)]. However, it was much easier to show that there are two dimerized singlet configurations which form the exact ground state of the Majumdar-Ghosh model, and to argue that other dimer-singlet configurations, generated by the allowed variations, will not be the eigenstates. We will do a similar exercise for H_0, showing that the four SS-VBC states are the only allowed dimer configurations in the ground state.

The block Hamiltonian $h_6=P^A P^B$ of a six-site plaquette is the basic building block of H_0. Since P^A and P^B are the spin projectors, the lowest energy of h_6 is zero. This corresponds to either P^A or P^B or both becoming zero in a given spin configuration of the block. This happens when the three A sublattice spins in a six-site plaquette form a total spin$=1/2$ state, or the same thing happens for B sublattice spins or for both. One way, in which this can be achieved, is by forming exactly one singlet bond out of three A or B sublattice spins of a plaquette. Thus a simple rule emerges for constructing the dimerized ground state of H_0. If a dimer configuration on the full square lattice is such that, on every six-site plaquette, there exists at least one singlet bond (dimer) between only A or only B sublattice spins, then all the plaquette Hamiltonians can be simultaneously satisfied (that is, every h_6 is in its ground state), and such a configuration will be an exact zero energy ground state of H_0.

Now, the number of rectangular plaquettes is equal to two times the number of sites, hence four times the number of dimers of any dimer covering of the lattice. Since a dimer belongs at most to four rectangles, to satisfy all rectangles simultaneously, each dimer should belong exactly to four rectangles, and each rectangle should contain a single dimer. Since a dimer constructed from third neighbors belongs to only two rectangles, such dimers have to be rejected, and one should only use diagonal dimers.

Let us now consider one diagonal dimer. The remaining sites of the square plaquette on which this dimer sits have to be part of a dimer. However, since two dimers cannot be on the same rectangular plaquette, the only possibility is that these dimers are perpendicular to the first one. This is precisely the prescription to construct a Shastry-Sutherland state. The freedom to chose the position and orientation of the first dimer leads to four different states. The exact diagonalization calculations on the 20 site and 32 site clusters presented in this paper support this assertion. Note that with periodic boundary conditions of length 4, a dimer constructed from third neighbors satisfies four rectangles, which leads to two additional ground states on the 16-site cluster.

[1] T. Senthil, A. Vishwanath, L. Balents, S. Sachdev, and M. P. A. Fisher, Science **303**, 1490 (2004).
[2] T. Senthil, L. Balents, S. Sachdev, A. Vishwanath, and M. P. A. Fisher, Phys. Rev. B **70**, 144407 (2004).
[3] L. D. Landau, E. M. Lifshitz, and E. M. Pitaevskii, *Statistical Physics* (Butterworth-Heinemann, New York, 1999).
[4] H. J. Schulz, T. A. L. Ziman, and D. Poilblanc, J. Phys. I **6**, 675 (1996).
[5] L. Capriotti, F. Becca, A. Parola, and S. Sorella, Phys. Rev. Lett. **87**, 097201 (2001).
[6] D. Poilblanc, E. Gagliano, S. Bacci, and E. Dagotto, Phys. Rev. B **43**, 10970 (1991).
[7] V. N. Kotov, J. Oitmaa, O. P. Sushkov, and Z. Weihong, Philos. Mag. A **80**, 1483 (2000).
[8] Rajiv R. P. Singh, Zheng Weihong, C. J. Hamer, and J. Oitmaa, Phys. Rev. B **60**, 7278 (1999).
[9] M. E. Zhitomirsky and K. Ueda, Phys. Rev. B **54**, 9007 (1996).
[10] L. Capriotti and S. Sorella, Phys. Rev. Lett. **84**, 3173 (2000).
[11] A. Kuklov, N. Prokof'ev, and B. Svistunov, Phys. Rev. Lett. **93**, 230402 (2004).
[12] J. Sirker, Z. Weihong, O. P. Sushkov, and J. Oitmaa, Phys. Rev. B **73**, 184420 (2006).
[13] F. Krüger and S. Scheidl, Europhys. Lett. **74**, 896 (2006).
[14] M. Mambrini, A. Läuchli, D. Poilblanc, and F. Mila, Phys. Rev. B **74**, 144422 (2006).
[15] L. Capriotti, F. Becca, A. Parola, and S. Sorella, Phys. Rev. B **67**, 212402 (2003).
[16] C. D. Batista and S. A. Trugman, Phys. Rev. Lett. **93**, 217202 (2004).
[17] A. W. Sandvik, Phys. Rev. Lett. **98**, 227202 (2007).
[18] B. S. Shastry and B. Sutherland, Physica B & C **108B**, 1069 (1981).
[19] F. D. M. Haldane, Phys. Rev. Lett. **61**, 1029 (1988).
[20] N. Read and S. Sachdev, Nucl. Phys. B **316**, 609 (1989).
[21] C. K. Majumdar and D. K. Ghosh, J. Math. Phys. **10**, 1399 (1969); C. K. Majumdar, J. Phys. C **3**, 911 (1970).
[22] D. J. Klein, J. Phys. A **15**, 661 (1982); J. T. Chayes, L. Chayes, and S. A. Kivelson, Commun. Math. Phys. **123**, 53 (1989).
[23] P. O. Löwdin, Rev. Mod. Phys. **36**, 966 (1964).
[24] S. Fujimoto, Phys. Rev. B **72**, 024429 (2005); K. S. Raman, R. Moessner, and S. L. Sondhi, *ibid.* **72**, 064413 (2005); Z. Nussinov, C. D. Batista, B. Normand, and S. A. Trugman, *ibid.* **75**, 094411 (2007).
[25] D. S. Rokhsar and S. A. Kivelson, Phys. Rev. Lett. **61**, 2376 (1988).
[26] K. Takano, J. Phys. A **27**, L269 (1994); B. Kumar, Phys. Rev. B **66**, 024406 (2002); N. Surendran and R. Shankar, *ibid.* **66**, 024415 (2002).
[27] B. Kumar, Phys. Rev. B **71**, 174434 (2005).
[28] A staggered dimer phase on the square lattice can alternatively be stabilized by positive cyclic ring-exchange interactions: A. Läuchli, J. C. Domenge, C. Lhuillier, P. Sindzingre, and M.

Troyer, Phys. Rev. Lett. **95**, 137206 (2005).
[29] B. Sutherland, Phys. Rev. B **37**, 3786 (1988).
[30] H. Neuberger and T. Ziman, Phys. Rev. B **39**, 2608 (1989).
[31] P. Hasenfratz and F. Niedermayer, Z. Phys. B: Condens. Matter **92**, 91 (1993).
[32] B. Bernu, C. Lhuillier, and L. Pierre, Phys. Rev. Lett. **69**, 2590 (1992).
[33] A. Läuchli, S. Wessel, and M. Sigrist, Phys. Rev. B **66**, 014401 (2002).
[34] I. Affleck, T. Kennedy, E. H. Lieb, and H. Tasaki, Phys. Rev. Lett. **59**, 799 (1987); I. Affleck, T. Kennedy, E. H. Lieb, and H. Tasaki, Commun. Math. Phys. **115**, 477 (1988).